A Preliminary Experimental Study on the Effects of Wear on the Torsional Stiffness of Strain Wave Gears

Terms of use:

(Article begins on next page)

17 April 2024

A Preliminary Experimental Study on the Effects of Wear on the Torsional Stiffness of Strain Wave Gears

Andrea Raviola *[ID], **Andrea De Martin** and **Massimo Sorli** [ID]

Department of Mechanical and Aerospace Engineering, Politecnico di Torino, Corso Duca degli Abruzzi 24, 10129 Torino, Italy
* Correspondence: andrea.raviola@polito.it

Abstract: Strain wave gears, also known as harmonic drives, are employed in a wide range of fields such as robotics and aerospace, where light weights, precision, and reliability are essential to the correct execution of the tasks. For this reason, their understanding and optimization are of high interest for both academia and industry. Previous studies have been mainly focused on investigating and modeling the working principle of strain wave gears in nominal operating conditions. On the contrary, the present paper describes the results of an experimental campaign aimed to introduce wear in gears of two different suppliers and its impact on the gear torsional stiffness. Results show how the change in the gear performance strongly depends both on the gear manufacturer and the location of wear. For the analyzed components, a damaged wave generator–flexspline interface reduces the gear stiffness up to one-fourth of its nominal value, while the non-nominal shape of the teeth jeopardizes the gearbox performance, leading up to just 4% of the nominal stiffness values, and resulting in backlash. Such data can be used to properly model the presence of wear in strain wave gears and to train data-driven diagnostics and prognostics routines to effectively detect such a fault.

Keywords: strain wave gears; harmonic drives; gearbox; wear; diagnostics; prognostics; modeling

1. Introduction

Strain wave gears (SWGs) are widely used in different fields and applications due to their compact and lightweight design, and ideally zero backlash, high position accuracy, and repeatability. Such gears are mainly composed of three components, as depicted in Figure 1.
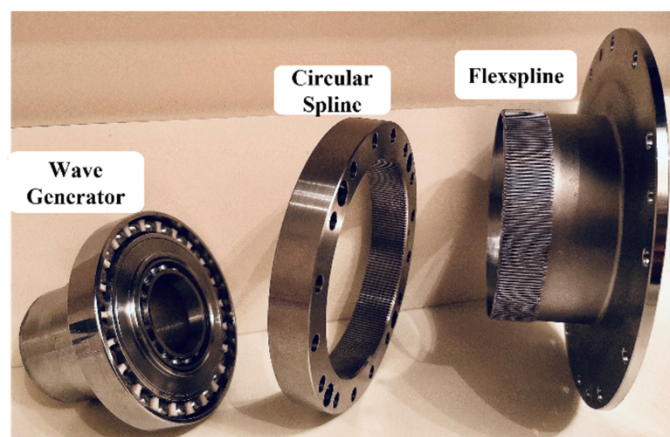
Figure 1. Main parts of a strain wave gear.

The wave generator (WG) is a flexible elliptical ball or roller bearing which, once inserted inside the flexspline (FS), a flexible gear with external toothing, elastically deforms

it, making it mesh with a rigid internal gear called circular spline (CS). In the present research campaign, each gear was assembled so that the wave generator is integral with the motor shaft, the flexspline is fixed, and the circular spline drives the output. Since these components are often integrated into machines requiring high precision and reliability, such as industrial manipulators [1,2], flight control servo-actuators, and spacecraft [3], their complete and accurate understanding is of primary importance. To do so, in the past years, several studies have been focused on developing high-fidelity models able to replicate key features such as kinematic error [4,5], hysteresis, and gear torsional stiffness [6–8]. More recent research also proposes a translation equivalent model of a SWG able to replicate the behavior of the gear subjected to wear [9]. Within this framework, the present paper describes the evolution of the performance drop over time of two strain wave gears tested on a dedicated test bench. According to the failure mode, effects, and criticality analysis (FMECA) reported in [10], even though wear has a low severity score, its high risk priority number is related to the fact that it will certainly occur within the component life. On the contrary, even though events such as flexspline fatigue fracture are critical in space applications [11], they can be difficult to detect or isolate and their occurrence can be minimized by the proper design of the gear [12,13]. Moreover, since wear can be generated by continuously running the gear within the manufacturer's specification, it is one of the simplest faults to introduce into the system. This approach prevents dismounting the group comprising the flexspline, circular spline, and output bearing, already assembled by the manufacturer, which would lead to the introduction of misalignments or eccentricities that could jeopardize the reliability of the measurements.

Among the multiple signals that can be obtained from the test bench through torque sensors and encoders, the authors decided to focus on the gear torsional stiffness. This choice was driven by the fact that other measurements often require specific operating conditions or load histories to be effectively measured. As an example, the kinematic error, defined as the mismatch between the expected and the actual angular output position, is a function of both angular velocity and load [4] and should be measured at a very low speed of the reducer [5]. As a result, it is difficult to quantify outside a dedicated experimental campaign. In addition, friction-related signals depend on the gear temperature and velocity, which can vary during typical tasks of the actuator, or could require specific command histories to be properly estimated [14]. In this scenario, accelerated life tests, such as the ones described in [15,16], are performed to evaluate the efficiency drop as a function of the number of revolutions. On the contrary, torque and torsion can be easily monitored, or estimated, during normal operations of the device on which the gear is mounted [17].

The novelty of the present research consists in highlighting the relationship between a progressive increment in wear and the resulting reduction in the torsional stiffness in strain wave gears. Results suggest the possibility of correlating the source and the magnitude of accumulated wear with changes in the trend of the gear torsional stiffness. This information can be crucial not only for gear manufacturers, helping them to know which elements need to be improved or redesigned, but also for researchers aiming to develop accurate models of such devices.

2. Hysteresis Curve of a Strain Wave Gear

The torsional stiffness of a strain wave gear can be derived by its hysteresis curve measured by locking the input shaft and by applying torque to the output. The measurement can be divided into three steps, which identify as many branches in which the hysteresis curve is divided:

1. Ramp-up branch: from zero torque and zero torsion, the output shaft is rotated until reaching a torque T equal to T_3, which is usually the gear rated torque or its repeatable peak torque. Since this part of the curve is not used for any calculation, it is omitted from Figures Figures 2a and b for clarity reasons.
2. Falling branch: from T_3 to $-T_3$.
3. Rising branch: from $-T_3$ to T_3.
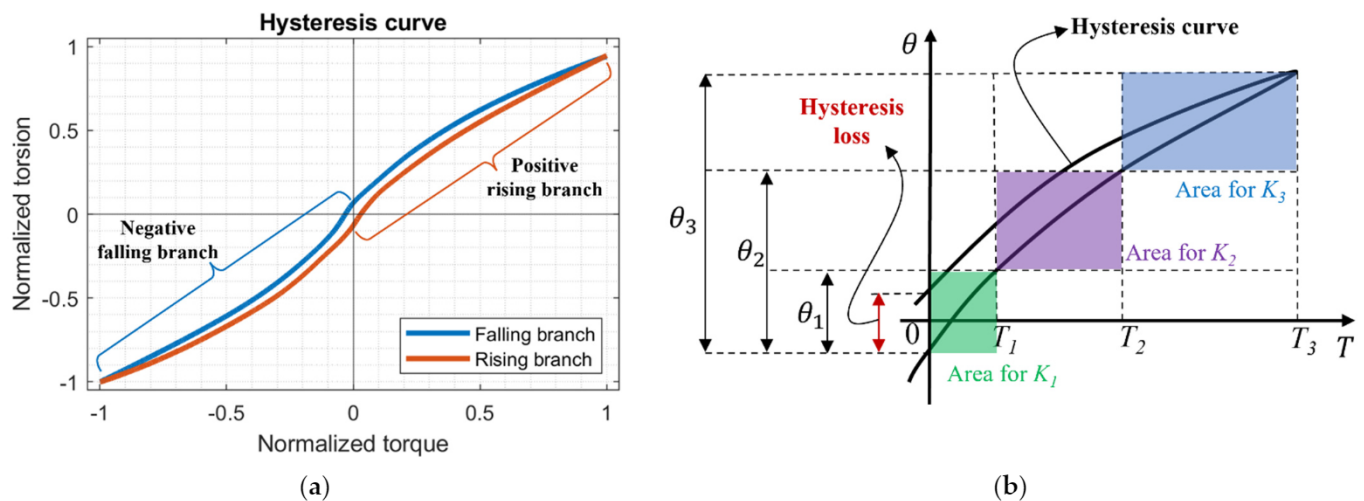
Figure 2. (**a**) Example of a normalized hysteresis curve of a strain wave gear. (**b**) Schematic representation of a hysteresis curve for a piecewise approximation of the gear torsional stiffness.

An example of a hysteresis curve of strain wave gear is reported in Figure 2a. Here, both torque (T) and torsion (θ) are normalized according to their maximum values T_3 and θ_3, respectively.

The torsional stiffness (K) of a strain wave gear can be derived using a piecewise linear approximation [8] of the positive rising and the negative falling branches of the hysteresis curve as a function of the actual transmitted torque (T) as:

$$\begin{cases} K_1 = \frac{T_1}{\theta_1} \ if \ T \le T_1 \\ K_2 = \frac{T_2 - T_1}{\theta_2 - \theta_1} \ if \ T_1 < T \le T_2, \\ K_3 = \frac{T_3 - T_2}{\theta_3 - \theta_2} \ if \ T_2 < T \le T_3 \end{cases} \tag{1}$$

where T_1, T_2, and T_3 are three output torques specified by the supplier, and θ_1, θ_2, and θ_3 are the corresponding torsion values. As is better highlighted in Section 4, this approach describes well the hysteresis curve only in nominal operating conditions, while it is not effective in the case of damaged gears since it neglects the detailed trend of the gear stiffness as a function of the torque or the torsion introduced in [1]. For this reason, instead of using only three values, the gear stiffness was obtained by calculating the slope of both the positive rising and the negative falling branches of the hysteresis curve reported in Figure 2a. As schematized in Figure 2b, normally only one of them (e.g., the positive rising branch) is used to derive the gear torsional stiffness. Nevertheless, in the present research, the negative falling branch was also considered. This was done to evaluate possible asymmetries in the behavior of the gear based on the direction of the applied load. Similar approaches can be also found in studies related to magnetism [18]. All measurements were performed under the same angular positions of both the wave generator and the circular spline to minimize the impact of changes in misalignments and eccentricities caused by manufacturing and assembly tolerances.

Additional useful data that can be extracted from a hysteresis curve are:

1. Hysteresis loss: defined as the torsion at zero torque, it is identified by the intersection between the hysteresis curve and the vertical axis ($T = 0$), as shown in Figure 2b.
2. Hysteresis area: area of the hysteresis loop delimited by the falling and the rising branches. This value is a measurement of the work dissipated by the system due to its torsion and friction losses. The higher the area, the lower the efficiency of the gearbox.
3. Maximum and minimum torsion: respectively, the highest and the lowest values of torsion measured when reaching the torque of $\pm T_3$.

3. Introduction of Wear in Strain Wave Gears

During the research campaign, several gears, from two different manufacturers and with a rated power of about 29 kW, were tested on a dedicated test bench similar to the ones described in [9,15]. A schematic representation of the connection among its parts is depicted in Figure 3. However, due to the consistency and the repeatability of the measurements, only the data from two gears, one from each supplier, are reported.
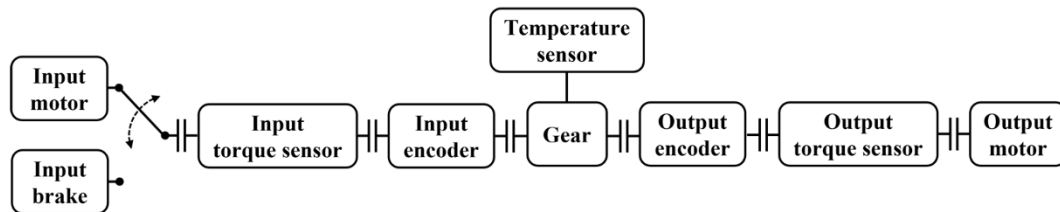

Figure 3. Schematic representation of the test bench used for testing strain wave gears.

The test bench was designed in a modular way to be able to run multiple tests according to the user's requirements. This easily allows switching from a setup where the input motor is used to run the gear at constant speed and torque, to one in which a brake system locks the gear input shaft for measuring its hysteresis curve. A measurement system collects data from input/output encoders and torque sensors at a frequency of 1 kHz. In addition, a temperature probe, attached to the gear output bearing, was used to ensure that all tests were executed within the temperature operating range defined by the manufacturer and that all measurements of the hysteresis curve were performed under the same conditions. The proposed setup allows running several tests without dismounting the gear or the sensors attached to it, avoiding introducing assembly errors in the system. The test campaign can be summarized in three main steps:

1. Measurement of the hysteresis curve to be used as a reference for the gear performance in nominal operating conditions (sample 1).
2. Run the gear within the manufacturer's load specifications to introduce wear into the system. In contrast to [9], here the gear was run in both clockwise and counterclockwise directions for an even distribution of wear on both sides of the flexspline and the circular spline teeth.
3. Measurement of the hysteresis curve to compare the degraded behavior of the gear with the reference values of step one (samples 2–5).

In the present study, steps two and three were repeated four times at regular intervals, leading to a total of five samples of the hysteresis curve for each strain wave gear. To avoid introducing undesired errors, steps 1 to 3 were executed sequentially, one gear at a time. Moreover, since the two gears are of the same size and, according to the manufacturers' specifications, present very similar behaviors, they were tested under the same operating conditions.

After testing, all gears were fully disassembled and inspected to better understand their health status and to investigate the root cause of their performance drop. From pictures in Figures 4 and 5, it can be seen how, despite being subjected to the same load history, the outcome is highly dependent on the supplier. For gear A, signs of pitting, highlighted with red circles in Figure 4a, started appearing on the flexspline teeth, while adhesive wear between the wave generator outer race and the flexspline inner surface [19] is visible in Figure 4b. On the contrary, the circular spline and the wave generator inner race barely presented any visible damage. Similar outcomes are reported in [15].
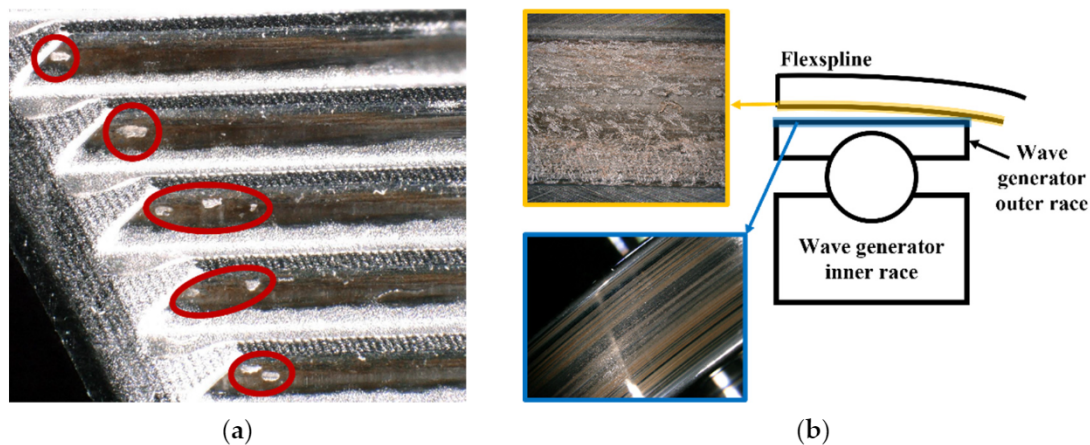
Figure 4. (**a**) Pitting on the flexspline teeth of gear A. (**b**) Adhesive wear marks on the wave generator and the flexspline of gear A.
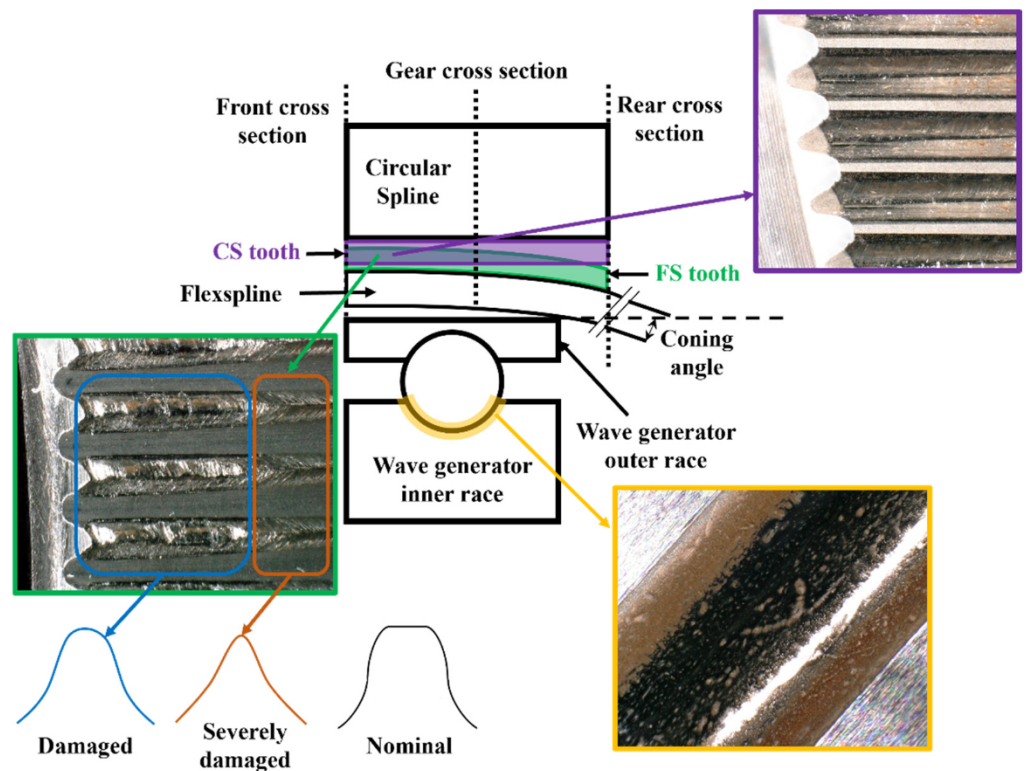
**Figure 5.** Effect of wear on the components of the strain wave gear B.

Different is the case of gear B, which shows higher accumulated damage. From pictures reported in Figure 5, it can be seen that, while the CS teeth present almost no wear marks, the FS ones are severely damaged. In addition, despite gear A, the wave generator inner race presents signs of fretting wear on both sides of the raceway.

As explained in [10], the different distribution of the tooth damage is related to the presence of the coning angle caused by the deformation of the flexspline while meshing with the circular spline. This also affects the gear lubrication which, if poor, highly reduces the life of the component [20]. However, in contrast with the results reported in [10], the damage accumulated along the length of the FS teeth is higher in proximity to the gear cross-section. This suggests the presence of higher contact forces in the middle section of the toothing, probably caused by the bending stiffness of both the FS cup and the WG outer ring, the presence of the WG spheres, and the axial forces acting on the elliptical bearing in the direction of the flexspline diaphragm [21].

Even though each manufacturer uses specific tooth profiles, strain wave gears mostly adopt double arc profiles, with [22] or without [23] a common tangent, due to their advantages in position accuracy, but with the drawback of high stress concentration [24]. Once the profile of the FS tooth is defined, the CS tooth is generated according to the approach described in [25]. Ideally, this provides conjugate meshing between the two gears and proper load distribution. However, this is true only in nominal operating conditions. As schematized in Figure 5, wear makes the shape of the FS tooth change from ideal to triangular, leading to backlash, which, as shown in [22,26], can compromise the proper functioning of the gear. Moreover, offsets from the nominal FS and CS teeth shapes highly affect the gear torsional stiffness, especially at low torques [27]. The difference between the damage faced by the FS and CS teeth could be related to the different materials from which these components are made. Another possibility could be related to the manufacturing process of the circular spline, which could lead to a hardening of its teeth, making them more resistant to wear and more aggressive on the FS teeth. According to [28], a potential solution for extending the flexspline fatigue life consists in fine particle peening of the tooth surface.

4. Results

Five measurements of the hysteresis curves, reported in Figures 6a and 7a, were acquired, at constant intervals, to better study the effect of cumulative wear on the gear performance. Each data point was normalized according to the maximum values (e.g., maximum torque and torsion) reached during the test campaign, which were different for gear A and gear B.
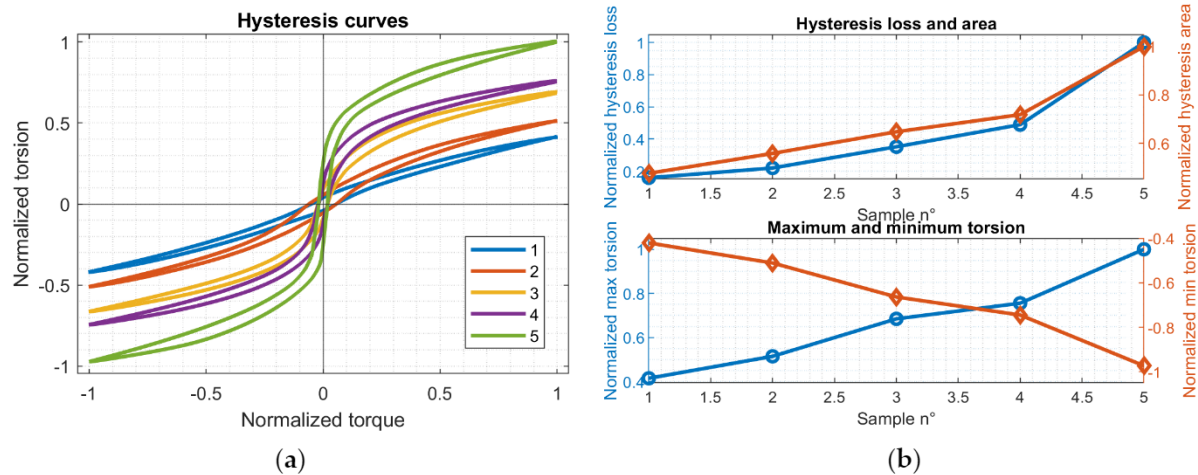

(a)   (b)
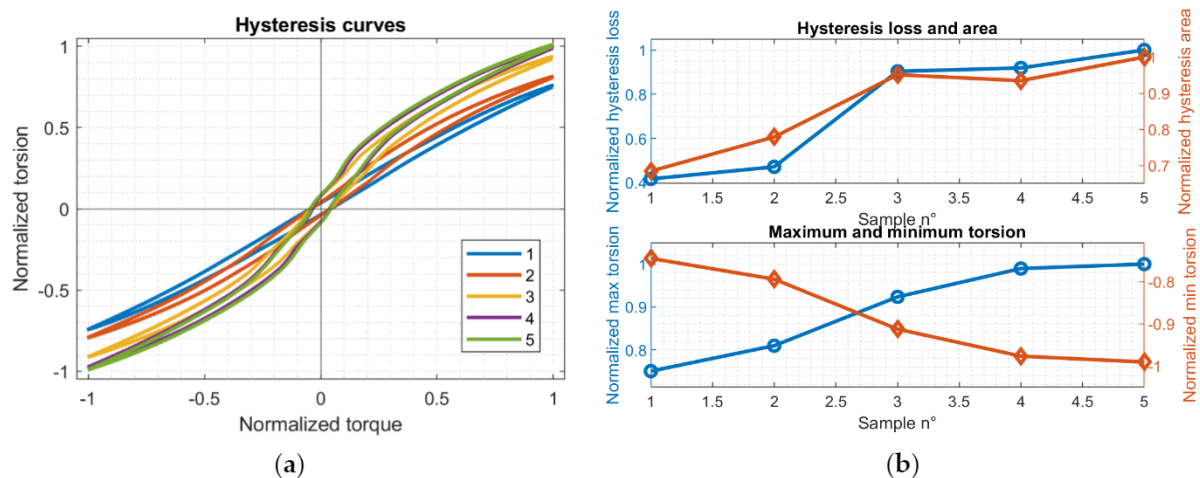
Figure 6. (**a**) Evolution of the hysteresis curve of gear A over time normalized with respect to the measurements in sample 5. (**b**) Trends of the hysteresis loss, area, and minimum and maximum torsion of gear A over time normalized with respect to the measurements in sample 5.

Based on the microscope pictures reported in Figure 4, it can be supposed that, for gear A, the changes among the hysteresis curves of Figure 6a are mostly related to the damaged WG–FS interface. The resulting sliding between the wave generator and the flexspline is likely to be the cause of the wavy trend of the hysteresis curve within ±20% of the highest torque reached during testing [11]. So, over time, the curve not only tends to rotate counterclockwise, showing a behavior typical of a cyclic softening, but also deforms and expands. This is visible from the first plot of Figure 6b, where both hysteresis loss and area increase. In more detail, it can be noted that the damage caused by wear is higher in the first half of the test (samples 1–3), with a +117% increment in the hysteresis loss, than in the second one (samples 3–5), where it settles around +11%. This shows that the majority of the damage appeared in the first half of the test campaign. On the contrary, an almost stable behavior of the gear is present in the second half, leading to three almost overlapped

hysteresis curves. The drop in the gear performance is also visible in Figure 6b through the increment of about 33% in both the minimum and the maximum gear torsion between initial and final working conditions, with a major variation (+23%) in the first half of the test for both directions of the applied load.

Figure 7. (**a**) Evolution of the hysteresis curve of gear B over time normalized with respect to the measurements in sample 5. (**b**) Trends of the hysteresis loss, area, minimum, and maximum torsion of gear B over time normalized with respect to the measurements in sample 5.

A similar analysis can be conducted for gear B. However, here, the hysteresis curves of Figure 7a show a different evolution over time.

The high damage faced by the flexspline teeth depicted in Figure 5 reduces the amount of simultaneously meshing teeth, leading to a S-shaped profile of the hysteresis curve. The high stretching of the curve, especially at low torques, is an indicator of the severity of the damage experienced by the FS teeth, which are not able to properly transmit torque through the system. This is also visible in Figure 7b, where the final value of the hysteresis loss is more than six times higher (+532%) than the one at the initial conditions, while the overall increment in both minimum and maximum torsion is about +141%. However, in contrast with gear A, the highest variations of hysteresis loss and area, respectively +184% and +54%, are nearer the end of the test campaign (samples 3–5) than the first half (+121% and +36%). In general, such different behavior between the two tested gears can be associated with the reduction in the number of meshing teeth. According to [29], in strain wave gears, the higher the number of meshing pairs, the greater the gear torsional stiffness. Nevertheless, the change in the shape of the FS teeth generates backlash in the transmission, requiring the gear higher torsion to transmit the desired torque. As depicted in Figure 4a, the toothing of gear A is still in good condition, while most of the damage is located at the WG–FS interface. The different evolution over time of the hysteresis curves between the two gears, together with the microscope examination of the damaged components, suggests the possibility of detecting the root cause of the failure mode. For both gears A and B, the accumulated damage caused by wear makes the hysteresis curve change, leading to mechanical relaxation and to a drop in the overall gear torsional stiffness. Since the hysteresis curve expresses a relationship between the input and the output of the device, the obtained values represent the overall gear torsional stiffness K. According to [30], this quantity can be also expressed as a series of three terms, leading to:

$$\frac{1}{K} = \frac{1}{K_{WG}} + \frac{1}{K_m} + \frac{1}{K_{FS}}, \qquad (2)$$

where K_{WG}, K_m, and K_{FS} are, respectively, the contributions to the gear stiffness (K) attributed to the wave generator, the FS–CS meshing, and the flexspline cup. Based on the failure modes depicted in Figures 4 and 5, such a distinction can be useful to properly

model degraded operating conditions of the gear by modifying the values of one or more terms of Equation (2). As an example, for gear B, most of the damage is associated with the flexspline teeth. This could be simulated by decreasing the value of K_m, while leaving the other two terms unaltered. On the contrary, for gear A, the performance drop is likely caused by the wear on the WG–FS interface, so only the term K_{WG} should be modified. Possible changes in the term K_{FS} could be driven by other failure modes, such as a crack on the flexspline cup [31].

The need to accurately simulate the presence of faults and failures of different origins and magnitudes is fundamental for the development of effective prognostics and health management routines. As proven in previous studies in fields such as robotics [32] and aeronautics [33,34], high-fidelity models can be adopted to create datasets of both healthy and faulty systems that are then used to train data-driven models for health features extraction. For this reason, a realistic description of the gear behavior is crucial to obtain reliable results. The same approach was adopted in [35], where an accelerated life test model for strain wave gears was based on a segmental stress history of the component. Within this framework, in the proposed study, the gear torsional stiffness was not simplified as in Equation (1), but was derived from the slope of the negative falling and the positive rising branches of the hysteresis curves of Figures 6a and 7a. The results are reported in Figure 8.
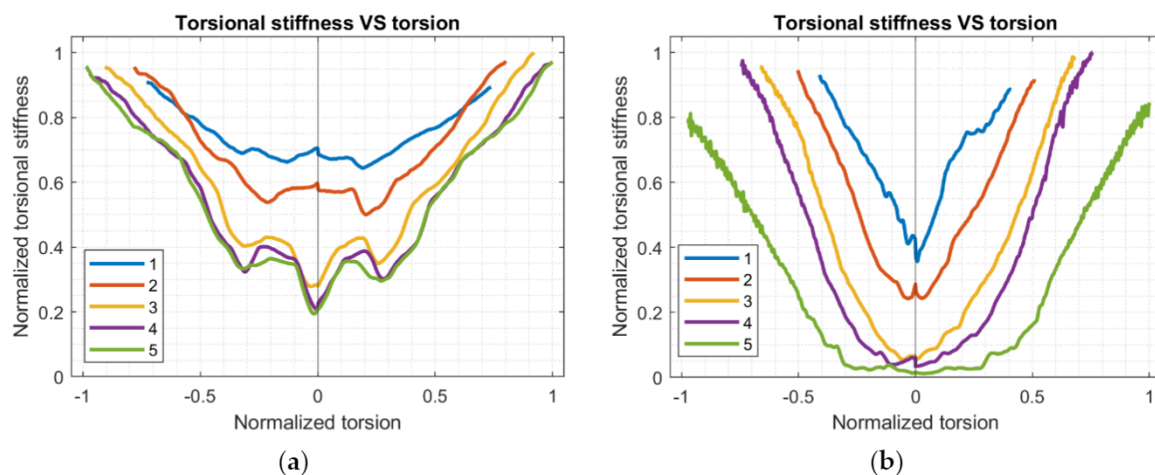
Figure 8. (**a**) Trends of the torsional stiffness as a function of torsion of gear A over time normalized with respect to the measurements in sample 5. (**b**) Trends of the torsional stiffness as a function of torsion of gear B over time normalized with respect to the measurements in sample 5.

Even though gears A and B show different behaviors, in both cases, the curves tend to shift towards the external region and the bottom of the graph. In the first scenario, the same level of the gear torsional stiffness is reached with an increasing value of torsion. This is caused by a degradation in the FS–CS meshing, which, over time, requires a higher torsion to transmit the same torque. Instead, the translation towards the bottom highlights a progressive reduction in the torsional stiffness under the same configuration of the gear. Such a difference is higher at low values of torsion, where there are fewer teeth simultaneously engaging. As an example, at zero torsion, the last measurement (sample 5) shows a stiffness value about 69% lower than the one during the nominal operating conditions for gear A, while the reduction is about 96% for gear B. The catastrophic drop in gear B, caused by the backlash between the teeth, goes on until about 30% of the maximum measured torsion, while the first consistent increment in the gear stiffness only appears at about 40% of it. It should be pointed out that, for the same torsion measurement, the maximum values of gear torsional were reached in nominal operating conditions.

As already mentioned, the different reduction in the torsional stiffness faced by gear A is related to the better status of its toothing. However, the damaged WG–FS interface is

likely the cause of the drop of between 20% and 28% of the maximum measured torsion, which corresponds to an average torque of about 12% of the maximum reached in the hysteresis curves in Figure 6a. This hypothesis is supported by the fact that the stiffness decrement is quite steep, leading to the assumption that it was caused by a sliding between the wave generator outer race and the flexspline inner surface.

5. Conclusions

In the proposed paper, the effects of wear on the torsional stiffness of two different strain wave gears are presented. The gears were run on a dedicated test bench within the manufacturers' load specifications and, at regular intervals, the hysteresis curve was sampled. From it, changes over time of specific parameters, such as the minimum and the maximum torsion, the hysteresis loss, and the gear stiffness, were derived. The extracted measurements, together with pictures of the damaged gears taken with a microscope, highlight the impact wear has on the overall behavior of a strain wave gear. The severity of this failure mode not only depends on the element of the gear that is most damaged, but also on the manufacturer. Based on the collected data, the FS–CS meshing stiffness (K_m) is the term mostly affected by the presence of wear. The proper meshing between the flexspline and the circular spline is fundamental for the correct functioning of the gear, especially at low torques. The presented findings show that both high-fidelity models and control algorithms should not only be tailored according to the supplier, but also developed based on both nominal and degraded operating conditions of the gear.

Future work will focus on studying the effect of wear on other signals that can be extracted from the gear test bench, such as efficiency and kinematic error. In addition, other failure modes, such as tooth and flexspline cracks, will be inserted in the system and their impact on the gear performance will be quantified.

References

1. Kircanski, N.M.; Goldenberg, A.A. An Experimental Study of Nonlinear Stiffness, Hysteresis, and Friction Effects in Robot Joints with Harmonic Drives and Torque Sensors. *Int. J. Robot. Res.* **1993**, *16*, 214–239. [CrossRef]
2. Zhao, J.; Yan, S.; Wu, J. Analysis of parameter sensitivity of space manipulator with harmonic drive based on the revised response surface method. *Acta Astronaut.* **2014**, *98*, 86–96. [CrossRef]
3. Ueura, K.; Kiyosawa, Y.; Kurogi, J.N.I.; Kanai, S.; Miyaba, H.; Maniwa, K.; Suzuki, M.; Obara, S. Development of strain wave gearing for space applications. In Proceedings of the 12th European Space Mechanisms & Tribology Symposium (ESMATS), Liverpool, UK, 19–21 September 2007; Volume 2007.
4. Ghorbel, F.H.; Gandhi, P.S.; Alpeter, F. On the kinematic error in harmonic drive gears. *J. Mech. Des. Trans. ASME* **2001**, *123*, 90–97. [CrossRef]
5. Zou, C.; Tao, T.; Jiang, G.; Zeng, P.; Du, H. Measurement and modeling of kinematic error and clearance in harmonic drives. In Proceedings of the Electronic and Information Technology Conference (JIMET 2015), Chongqing, China, 18–20 December 2015; pp. 102–109.
6. Ruderman, M.; Bertram, T.; Iwasaki, M. Mechatronics Modeling, observation, and control of hysteresis torsion in elastic robot joints. *Mechatronics* **2014**, *24*, 407–415. [CrossRef]
7. Dhaouadi, R.; Ghorbel, F.H.; Gandhi, P.S. A New Dynamic Model of Hysteresis in Harmonic Drives. *IEEE Trans. Ind. Electron.* **2003**, *50*, 1165–1171. [CrossRef]
8. Zhang, H.; Ahmad, S.; Liu, G.; Member, S. Modeling of Torsional Compliance and Hysteresis Behaviors in Harmonic Drives. *IEEE/ASME Trans. Mechatron.* **2015**, *20*, 178–185. [CrossRef]

9. Tang, T.; Jia, H.; Li, J.; Wang, J.; Zeng, X. Modeling of transmission compliance and hysteresis considering degradation in a Harmonic drive. *Appl. Sci.* **2021**, *11*, 665. [CrossRef]
10. Raviola, A.; De Martin, A.; Guida, R.; Jacazio, G.; Mauro, S.; Sorli, M. Harmonic Drive Gear Failures in Industrial Robots Applications: An Overview. In Proceedings of the 6th European Conference of the Prognostics and Health Management Society, Online, 28 June–2 July 2021.
11. Schafer, I.; Bourlier, P.; Hantschack, F.; Roberts, E.W.; Lweis, S.D.; Forster, D.J.; John, C. Space lubrication and performance of harmonic drive gears. In Proceedings of the 11th ESMATS Symposium, Lucerne, Switzerland, 21–23 September 2005.
12. Lewicki, D.G. Gear crack propagation path studies-guidelines for ultra-safe design. *J. Am. Helicopter Soc.* **2002**, *47*, 64–72. [CrossRef]
13. Lewicki, D.G.; Ballarini, R. Effect of Rim Thickness on Gear Crack Propagation Path. *J. Mech. Des. Trans. ASME* **1997**, *119*, 88–95. [CrossRef]
14. Raviola, A.; Guida, R.; Sorli, M.; De Martin, A.; Pastorelli, S.; Mauro, S. Effects of Temperature and Mounting Configuration on the Dynamic Parameters Identification of Industrial Robots. *Robotics* **2021**, *10*, 83. [CrossRef]
15. Li, J.Y.; Wang, J.X.; Zhou, G.W.; Pu, W.E.I.; Wang, Z.H. Accelerated life testing of harmonic driver in space lubrication. *Proc. Inst. Mech.Eng. Part J J. Eng.Tribol.* **2015**, *229*, 1491–1502. [CrossRef]
16. Zhu, Y.; Elsayed, E.A. Design of accelerated life testing plans under multiple stresses. *Nav. Res. Logist.* **2013**, *60*, 468–478. [CrossRef]
17. Madsen, E.; Rosenlund, O.S.; Brandt, D.; Zhang, X. Model-based on-line estimation of time-varying nonlinear joint stiffness on an e-series universal robots manipulator. In Proceedings of the 2019 International Conference on Robotics and Automation (ICRA), Montreal, QC, Canada, 20–24 May 2019; pp. 8408–8414. [CrossRef]
18. Jackson, M.; Solheid, P. On the quantitative analysis and evaluation of magnetic hysteresis data. *Geochem. Geophys. Geosystems* **2010**, *11*, 1–25. [CrossRef]
19. Ueura, K.; Kiyosawaa, Y.; Kurogi, J.; Kanai, S.; Miyaba, H.; Maniwa, K.; Suzuki, M.; Obara, S. Tribological aspects of a strain wave gearing system with specific reference to its space application. *Inst. Mech. Eng. Part J: J. Eng. Tribol.* **2008**, *222*, 1051–1061. [CrossRef]
20. Routh, B.; Maiti, R.; Ray, A.K. Analysis of coning and lubrication at flexspline cup and cam interface in conventional harmonic drives. *Ind. Lubr. Tribol.* **2017**, *69*, 817–827. [CrossRef]
21. Roberts, E.W.; Bridgeman, P.; Jansson, M.; Schulke, M.; Tvaruzka, A. The Performance and Life of Fluid-Lubricated Harmonic Drive®Gears. *ESMATS* **2015**, *2015*, 23–25.
22. Chen, X.; Liu, Y.; Xing, J.; Lin, S.; Xu, W. The parametric design of double-circular-arc tooth profile and its influence on the functional backlash of harmonic drive. *Mech. Mach. Theory* **2014**, *73*, 1–24. [CrossRef]
23. Yang, Y.; Li, J.; Wang, J.; Zeng, F. Analysis of Tooth Profile Modification and Meshing Characteristics of Double Arc Harmonic Drive. In Proceedings of the 2021 4th International Conference on Electron Device and Mechanical Engineering (ICEDME), Guangzhou, China, 19–21 March 2021; pp. 268–273. [CrossRef]
24. Kayabasi, O.; Erzincanli, F. Shape optimization of tooth profile of a flexspline for a harmonic drive by finite element modelling. *Mater. Des.* **2007**, *28*, 441–447. [CrossRef]
25. Chen, G.; Li, H.; Liu, Y. Double-arc harmonic gear profile design and meshing analysis for multi-section conjugation. *Adv. Mech. Eng.* **2019**, *11*, 1–14. [CrossRef]
26. Guida, R.; Raviola, A.; Migliore, D.F.; De Martin, A.; Mauro, S.; Sorli, M. Simulation of the Effects of Backlash on the Performance of a Collaborative Robot: A Preliminary Case Study. *Mech. Mach. Sci.* **2022**, *120*, 28–35.
27. Hrcek, S.; Brumercik, F.; Smetanka, L.; Lukac, M.; Patin, B.; Glowacz, A. Global Sensitivity Analysis of Chosen Harmonic Drive Parameters Affecting Its Lost Motion. *Materials* **2021**, *14*, 5057. [CrossRef] [PubMed]
28. Zhang, B.; Wei, P.; Liu, H.; Yan, H.; Guagliano, M. Effect of fine particle peening on surface integrity of flexspline in harmonic drive. *Surf. Coat. Technol.* **2022**, *433*, 128133. [CrossRef]
29. Ma, J.; Li, C.; Luo, Y.; Cui, L. Simulation of meshing characteristics of harmonic reducer and experimental verification. *Adv. Mech. Eng.* **2018**, *10*, 1–9. [CrossRef]
30. Zou, C.; Tao, T.; Jiang, G.; Mei, X.; Wu, J. A harmonic drive model considering geometry and internal interaction. *Proc. Inst. Mech. Eng. Part. C J. Mech. Eng. Sci.* **2017**, *231*, 728–743. [CrossRef]
31. Li, S. Diaphragm stress analysis and fatigue strength evaluation of the flex-spline, a very thin-walled spur gear used in the strain wave gearing. *Mech. Mach. Theory* **2016**, *104*, 1–16. [CrossRef]
32. Grosso, L.A.; De Martin, A.; Jacazio, G.; Sorli, M. Development of data-driven PHM solutions for robot hemming in automotive production lines. *Int. J. Progn. Health Manag.* **2020**, *11*, 1.
33. Bertolino, A.C.; De Martin, A.; Jacazio, G.; Sorli, M. A case study on the detection and prognosis of internal leakages in electro-hydraulic flight control actuators. *Actuators* **2021**, *10*, 215. [CrossRef]
34. Bacci, A.; Bertolino, A.C.; De Martin, A.; Sorli, M. Multiphysics modeling of a faulty rod-end and its interaction with a flight control actuator to support phm activities. In Proceedings of the ASME International Mechanical Engineering Congress and Exposition, Proceedings (IMECE), Virtual, 1–4 November 2021; Volume 7B-2021, pp. 1–10.
35. Zhang, C.; Wang, S.; Wang, Z.; Wang, X. An accelerated life test model for harmonic drives under a segmental stress history and its parameter optimization. *Chin. J. Aeronaut.* **2015**, *28*, 1758–1765. [CrossRef]